

1 **The Malta-Sicily Escarpment: Mass movement**
2 **dynamics in a sediment-undersupplied margin.**
3

4 **Aaron Micallef^{1,2}, Aggeliki Georgiopoulou³, Timothy Le Bas⁴,**
5 **Joshu Mountjoy⁵, Veerle Huvenne⁴ and Claudio Lo Iacono^{4,6}**

6
7 1 University of Malta, Malta, aaron.micallef@um.edu.mt

8 2 GRC Geociències Marines, Universitat de Barcelona, Spain

9 3 University College Dublin, Ireland

10 4 National Oceanography Centre, UK

11 5 National Institute of Water and Atmospheric Research, New Zealand

12 6 Institut de Ciències del Mar, CSIC, Spain

13

14 **Abstract**

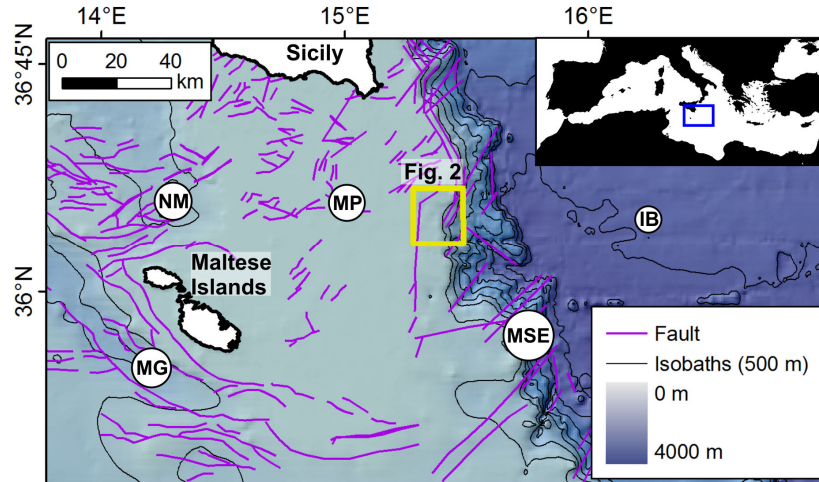
15
16 The Malta-Sicily Escarpment (MSE) is a steep carbonate escarpment that appears
17 to have largely remained isolated from inputs of fluvial and littoral sediments
18 since the Messinian Salinity Crisis. Mass movement activity has so far only been
19 inferred from sediment cores at the base of the MSE. In this study we use geo-
20 physical and sedimentological data acquired from the upper MSE and outer Malta
21 Plateau to: (i) map and characterise the dominant forms of mass movements, and
22 (ii) determine the nature and origin of these mass movements, and their role in the
23 evolution of the MSE. We document 67 mass movement scars across 370 km² of
24 seafloor. Slope instability entailed translational slides, spreads and debris flows
25 that mobilised Plio-Pleistocene outer shelf hemipelagic/pelagic sediments or car-
26 bonate sequences across the upper continental slope. Slope failure events are
27 caused by loss of support associated with the formation of channels, gullies, can-
28 yon heads and fault-related escarpments. Mass movements play a key role in erod-
29 ing the seafloor and transferring material to the lower MSE. In particular, they
30 control the extent of headward and lateral extension of submarine canyons, facili-
31 tate tributary development, remove material from the continental shelf and slope,
32 and feed sediment and drive its transport across the submarine canyon system.
33
34

35 **Keywords:** submarine mass movement, submarine canyon, sediment-
36 undersupplied margin, Malta-Sicily Escarpment, Mediterranean.

37 **1. Introduction**

38 The Malta-Sicily Escarpment (MSE) is one of the principal physiographic ele-
39 ments of the central Mediterranean (Fig. 1). Consisting of a steep, NNW-SSE
40 trending slope that extends southwards from the east coast of Sicily, the escarp-
41 ment is 250 km long and has a vertical relief of almost 3 km. The MSE is the ex-
42 pression of a passive margin separating the continental crust of the Malta Plateau
43 from the oceanic crust of the Ionian Basin (Argnani and Bonazzi 2005). Triassic-
44 Neogene sedimentary and volcanic sequences outcrop along the escarpment
45 (Casero et al. 1984; Scandone et al. 1981). Reconstructions of past sea level
46 changes (Imbrie et al. 1989) and stratigraphic analyses (Max et al. 1993; Osler and
47 Algan 1999) suggest that, following the Messinian Salinity Crisis (~5.9 Ma), the
48 majority of the MSE has largely remained isolated from inputs of fluvial and litto-
49 ral sediments, and that it has experienced low sedimentation rates; the escarpment
50 may thus be classified as a sediment-undersupplied margin. The MSE is also lo-
51 cated at the convergence between the eastward flowing Atlantic Ionian Stream and
52 the westward passage of the denser Levantine Intermediate Water. Sediment drift
53 accumulations, indicative of bottom current activity, have been reported at the foot
54 of the MSE (Marani et al. 1993)

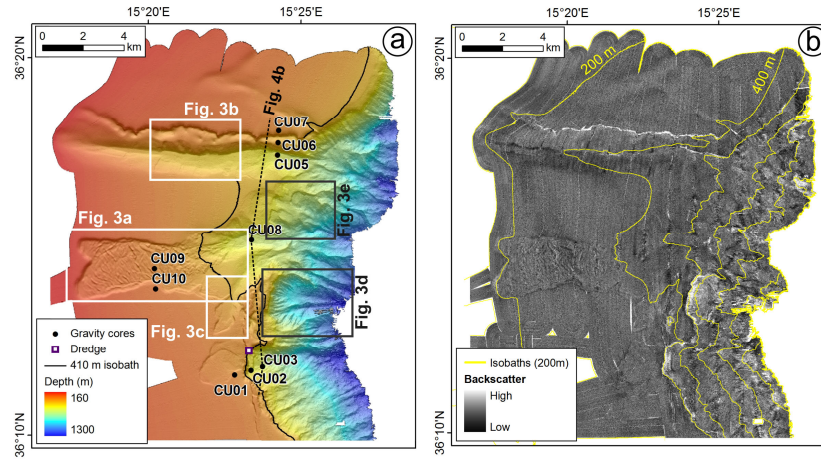
55 The role of slope instability in the overall evolution of the MSE is not well-
56 understood. Mass movement activity has mainly been inferred from sediment
57 cores. Volcaniclastic and terrigenous turbidites and debrites have been reported
58 from the lower reaches of a submarine canyon system that incises the MSE
59 (Casero et al. 1984; Scandone et al. 1981). Slumping across the MSE itself has
60 only been reported from seismic reflection profiles (Jongsma et al. 1985). In this
61 study we use geophysical and sedimentological data recently acquired from the
62 outer Malta Plateau and upper MSE to: (i) map and characterise the dominant
63 forms of mass movements, and (ii) determine the nature and origin of these mass
64 movements, and their role in the evolution of the MSE.
65



66
67
68
69
70
71
Fig. 1. Bathymetric map of the MSE, central Mediterranean Sea, showing the principal morphological features of the region (IB = Ionian Basin; MG = Malta Graben; MP = Malta Plateau; MSE = Malta-Sicily Escarpment; NM = North Malta Basin) (Source: IOC et al. (2003)). Faults are mapped from published seismic reflection data; some of them have been reactivated in the early Pliocene (Casero et al. 1984; Gardiner et al. 1995).

72 2. Data and methods

73 Our study is based on four types of data acquired from the MSE during the CU-
74 MECS research cruise (2012).
75 i. Multibeam echosounder (MBES) data: An area of $\sim 370 \text{ km}^2$ of seabed was sur-
76 veyed using a Kongsberg-Simrad EM-710 system (70-100 kHz) (Fig. 1). Both
77 bathymetry and backscatter grids with $10 \text{ m} \times 10 \text{ m}$ bin size were derived (Fig. 2).
78 These grids were visually interpreted and standard morphometric attributes (gradi-
79 ent, aspect, curvature) were extracted.
80 ii. Sub-bottom profiles: 500 km of high resolution seismic reflection profiles were
81 acquired simultaneously with the MBES data. The profiles were collected using a
82 hull-mounted CHIRP-II profiler with operating frequencies of 2-7 kHz. For con-
83 version of two-way travel time to depth we used a standard seismic p-wave veloc-
84 ity of 1600 m s^{-1} .
85 iii. Gravity cores: A total of 28 m of sediment cores were obtained from nine sites
86 using a 6-m gravity corer (Fig. 2a). The cores were visually logged, photographed,
87 and analysed in terms of sediment colour, magnetic susceptibility, p-wave veloc-
88 ity, and gamma density using a Geotek[®] Multi-Sensor Core Logger.
89 iv. Dredge samples: Samples were acquired with a cylindrical metallic dredge
90 from one selected site at a depth of 320 m (Fig. 2a).

91
92

93

94 Fig. 2. (a) Bathymetric data draped on a shaded relief map and (b) backscatter map of the study
95 area (isobaths at 200 m intervals). Location in Fig. 1.

96 3. Results

97 3.1 Seafloor morphology and composition

98 The study area comprises two morphologically diverse provinces (outer Malta Pla-
99 teau and MSE) that are divided by the 410 m isobath (Fig. 2a).

100 3.1.1 Outer Malta Plateau

101 The seafloor between 160 m and 410 m depth is predominantly smooth, very gen-
102 tly sloping (0.8° - 1.8°) towards the east, and characterised by low backscatter re-
103 sponse. Across the Outer Malta Plateau we identify three morphological elements
104 of interest:

105 (i) Escarpments

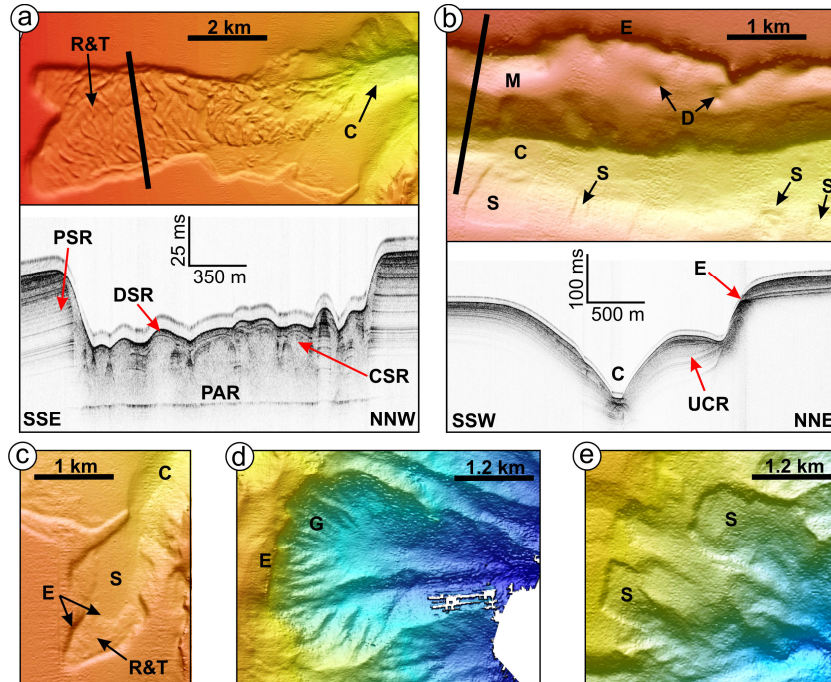
106 Steep breaks of slope, up to 12.5 km long and 60 m high, occur in three orienta-
107 tions: W-E, N-S and SW-NE. They are straight to non-linear, and they generally
108 correspond to high backscatter (Figs. 2; 3b).

109 (ii) Scars

110 Located just upslope of the 410 m isobath are four scars that range from 1 to 18
111 km² in area. The scars have ellipsoidal to elongated plan-form shapes oriented east
112 to north-eastwards; their lateral and upslope limits are characterised by escarp-
113 ments with gradients of up to 15° and heights of up to 50 m. The largest scar com-
114 prises a series of sub-parallel linear ridges and troughs (Fig. 3a). The other three
115 scars, on the other hand, are intersected by gently-sloping escarpments (Fig. 3c).
116 The downslope section of these scars consists of smooth, near-planar seafloor
117 whereas the upslope section comprises a ridge and trough pattern (Figs. 3a,c). The
118 downslope limit of all the scars is contiguous with another scar, a channel or an
119 escarpment.

120 (iii) Channels

121 The deepest part of the Outer Malta Plateau is incised by four channels. Two other
122 channels connect scars with the upper MSE (Figs. 3a, c). The longest channel (12
123 km long) dominates the northern part of the study area (Fig. 3b). Its steeper north-
124 ern wall is characterised by an elongated mounded morphology, up to 1 km wide,
125 which extends along the foot of a 70 m high escarpment. Two 90 m wide circular
126 depressions are also observed in that location. The walls of the long channel are
127 affected by sixteen small scars (0.03 – 0.4 km² in area), all of which slope towards
128 and connect to the channel bed. The scars are shallow (maximum depth of 5 m),
129 smooth, planar and have low aspect ratios.
130



131

132 Fig. 3. Bathymetric map and sub-seafloor image of the: (a) Largest scar in the Outer Malta Plateau;
 133 (b) Longest channel in the Outer Malta Plateau, the elongated morphology and escarpment
 134 across its northern wall. Bathymetric map of (c) Small scar in Outer Malta Plateau; (d) Amphitheatre-shaped depression in the upper MSE; (e) Shallow scars in the upper MSE. Depth legend
 135 in Fig. 2. Abbreviations: C = channel; CSR = chaotic seismic reflections; D = circular depressions; E = escarpment; G = gullies; M = mounded morphology; PAR = planar high amplitude reflector; PSR = parallel seismic reflections; R&T = ridges & troughs; S = scar; UCR = upwardly-convex high amplitude reflectors.
 136
 137
 138
 139

140 3.1.2 Upper MSE

141 The seafloor deeper than 410 m is considerably different from that upslope. The
 142 slope is steeper (mean gradient of 11°) and is heavily incised by a dense network
 143 of gullies and distinct larger and wider channels that extend all the way from the
 144 shelf break to the limit of data coverage (Fig. 2). The gullies have steep sidewalls
 145 and sharp interflues, whilst their beds generally coincide with high backscatter
 146 values. Some gullies are carved into large amphitheatre-shaped depressions (Fig.
 147 3d), the upslope limits of which are high escarpments (up to 150 m in height) that
 148 have a very high backscatter response (Fig. 2b). The southernmost of these de-

149 pressions intersects a N-S trending ridge; dredged material from this ridge consists
 150 of hard carbonate rocks. A large proportion of the gullied slope is affected by num-
 151 erous, shallow scars (Fig. 3e). These are oriented downslope with a predomi-
 152 nantly elongate plan shape, and they have upslope limits that are generally linear,
 153 steep and have a high backscatter character. The lower limit is difficult to identify
 154 from the bathymetric data. The scars are mostly located upslope or adjacent to gul-
 155 lies and channels.

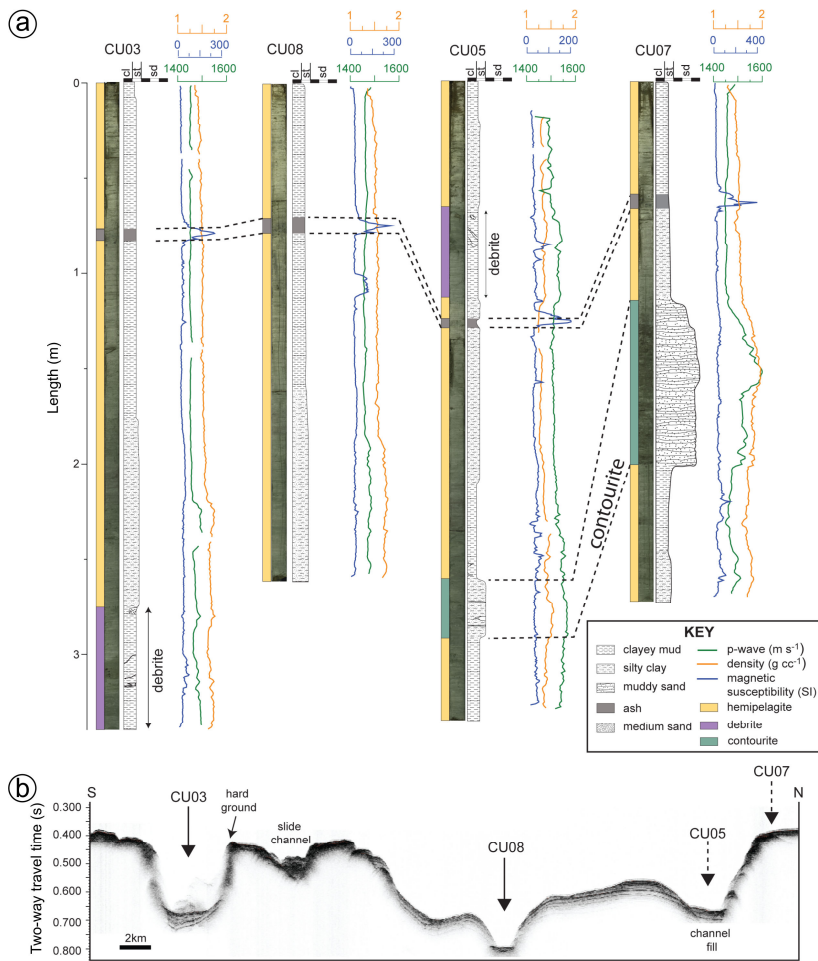
156 **3.2 *Sub-seafloor architecture***

157 The seismic expression of the sub-seafloor in most of the shallow province com-
 158 prises a sequence of continuous, parallel, high amplitude seismic reflections that is
 159 at least 50 m thick in places. At abrupt changes in slope, the sequence thins and
 160 seismic reflections converge. Sub-bottom profiles across scars in the shallow
 161 province show that this parallel seismic reflection pattern is truncated at escarp-
 162 ments (Fig. 3a). At the downslope limit of the scars, the seismic signature is pre-
 163 dominantly chaotic. Where ridge and trough morphology occurs, the seismic pat-
 164 tern is predominantly represented by an irregular, chaotic, low reflectivity unit,
 165 which has variable thickness and is draped by an up to 5 m thick unit of coherent,
 166 moderate reflectors (Fig. 3a). The base of the irregular unit is a planar, high ampli-
 167 tude reflector.
 168 The internal stratigraphy of the elongated mound on the long channel's northern
 169 wall is characterised by an asymmetric package of sub-parallel, upwardly-convex,
 170 high-amplitude reflectors (Fig. 3b). This sequence is also draped by a coherent,
 171 moderately reflective, 5 m thick unit.

172 **3.3 *Sub-surface sedimentology***

173 The sediment in all nine gravity cores is predominantly clay to silty clay of homo-
 174 geneous lithology and physical properties, and punctuated by infrequent variations
 175 (Fig. 4). These include:
 176
 177 i. Between 60 and 75 cm downcore in most cores, there is a layer of vol-
 178 canic ash that generates a characteristic high peak in the magnetic sus-
 179 ceptibility curve, which is used to correlate cores. This peak is found
 180 deeper downcore in core CU05, at about 120 cm.
 181 ii. The last 60 cm of core CU03 shows inclined laminae, sand clasts and er-
 182 ratic variability of the physical properties. Similar characteristics are
 183 found between 70 and 120 cm downcore in core CU05, 10 cm above the
 184 ash layer.

- 185 iii. Between 260 and 290 cm downcore in CU05 there is a sequence of silty
 186 clay containing medium sand laminae alternating with clay laminae,
 187 characterised by relatively higher gamma ray density and p-wave veloc-
 188 ity.
 189 iv. A 1 m thick sequence of unsorted, roughly-graded, medium to fine sand
 190 intermixed with clay occurs in core CU07. This sequence is characterised
 191 by relatively higher gamma ray density and p-wave velocity than the rest
 192 of the core, which correlates with the layer described above in core
 193 CU05.
 194



195 Fig. 4. (a) Data and interpretation of sediment cores from sites CU03, CU08, CU05, and (b) their location on a sub-seafloor transect. The coloured bar to the left of the core photo-
 196 graphs represents lithological interpretation. Location of cores and transect in Fig. 2a.
 197
 198

199 4. Discussion and conclusions

200 4.1 *Nature of mass movements and sediment transport*

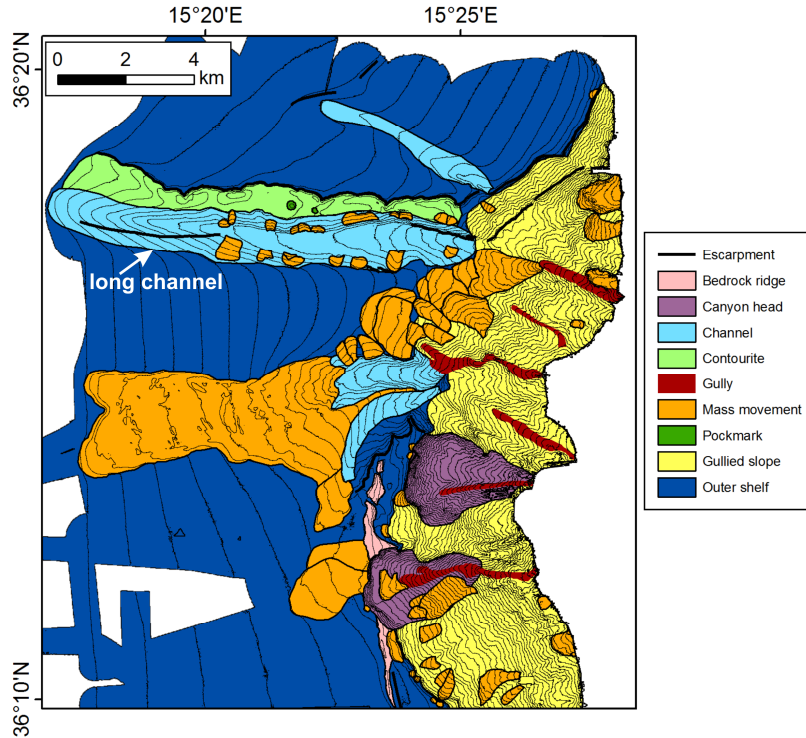
201 We interpret the scars documented across the study area as evidence of wide-
202 spread slope instability. The 67 mass movements identified can be divided into
203 two classes - shelf mass movements that affect the outer Malta Plateau, and slope
204 mass movements that occur across the MSE. Their areal extents range across three
205 orders of magnitude and display up to three levels of retrogression.

206 On the outer Malta Plateau, mass movements have occurred on very gentle slopes
207 of stratified fine sediments, which is likely of hemipelagic and pelagic origin and
208 deposited during the Plio-Pleistocene (Micallef et al. 2011; Tonarelli et al. 1993).
209 The style of deformation observed is indicative of both translational slides and debris
210 flows. The ridge and trough morphology is the signature of spreading, which
211 involves extension of a sediment unit and its break up into blocks that slide above
212 a planar failure surface (Micallef et al. 2007). Spreading occurs in the largest scar
213 as well as in the upslope sections of the smaller scars located at the shelf break.
214 The chaotic seismic signature of the downslope limit of the scars is indicative of
215 internal deformation, most likely caused by the occurrence of debris flows. The
216 core retrieved from the long channel thalweg (CU05) has a sequence with the de-
217 formed sediments and erratic physical properties (Fig. 4), which we interpret as a
218 debrite.

219 On the upper part of the MSE, slope instability has taken place in carbonate se-
220 quences with a steeply inclined exposure (Scandone et al. 1981). Due to the com-
221 position of the failed material, the chaotic seismic signature of the deposits, and
222 their linear to arcuate steep headwalls, we infer that the style of failure was either
223 a translational slide or debris avalanche (e.g. ten Brink et al. 2006). The amphi-
224 theatre-shaped depressions are likely canyon heads that result from coalescing, ar-
225 cuate scars (Mulder et al. 2012). Mass movements associated with the upslope de-
226 velopment of the southernmost of these canyon heads were powerful enough to
227 erode a structurally-controlled bedrock ridge at its headwall (Fig. 5).

228 From the geophysical and sediment core data in Figs. 3b and 4, we interpret the
229 elongated mounded morphology along the northern wall of the long channel as a
230 contourite (Rebesco and Stow 2001; Stow et al. 2002).

231
232



233
234

Fig. 5. Interpretation map of the study area (isobaths at 25 m intervals).

235 4.2 Causes of slope instability

236 We propose four potential causes of slope instability across the outer Malta Pla-
237 teau and upper MSE:
238

- 239 i. **Loss of support:** The retrogressive nature of the mass movements – with
240 their location upslope of other mass movements, escarpments, chan-
241 nel/gully beds or canyon heads - indicates that loss of support plays an
242 important role in triggering slope instability in the study area. Across the
243 MSE, the incision of gullies and channels triggers slope failures across
244 their walls due to oversteepening and loss of support (e.g. Micallef et al.
245 2012). These flank failures are responsible for widening and extending
246 the gullies and channels upslope. The same dynamics characterise the
247 long channel in the outer Malta Plateau. In this case, the formation of a

- 248 contouritic drift on the northern wall indicates that bottom currents may
 249 play a role in channel incision. Otherwise, loss of support is the result of
 250 a mass movement taking place downslope or associated with the upslope
 251 development of a submarine canyon head.
- 252 ii. **Sedimentation:** Hemipelagic and pelagic sedimentation, as well as con-
 253 touritic deposition along the northern wall of the long channel, provide
 254 the material that fails across the outer Malta Plateau. Sedimentation rates
 255 across the Malta Plateau in the last 5 Ma are reported to be low, in the
 256 range of ~6 cm per 1000 yr on the Malta Plateau (Max et al. 1993; Osler
 257 and Algan 1999). Thus, we believe that sediment loading and associated
 258 excess pore pressure development are not a pre-conditioning factor for
 259 slope instability in the region.
- 260 iii. **Faulting and seismicity:** Faults, linked to the different rates of under-
 261 thrusting between the buoyant Malta Plateau and the Ionian crust (Adam
 262 et al. 2000; Grasso 1993), are common across the study area (as shown in
 263 Fig. 1 and inferred from the escarpments in Fig. 5) and likely to have ex-
 264 erted a predominant control on the physiography and, indirectly, on the
 265 location of mass movements (e.g. occurrence of steep slope gradients,
 266 seafloor deformation, escarpments, and channels). Seismic activity has
 267 mostly been restricted to the northern section of the MSE (Argnani and
 268 Bonazzi 2005). Ground shaking associated with distal earthquakes could
 269 thus have played a minor role in triggering slope instability across the
 270 study area.
- 271 iv. **Fluid flow:** Deep fluid flow systems, sourced by Late Mesozoic sedi-
 272 mentary units, have been reported in parts of the outer Malta Plateau
 273 (Micallef et al. 2011). Fluid, likely transferred to the surface by faults in
 274 the Tertiary carbonate sequences, may thus play a role in reducing the
 275 stability of the outer Malta Plateau by elevating pore pressures in the
 276 sediments. The circular depressions identified on the northern wall of the
 277 long channel may be evidence of fluid escape at the seabed.

278 *4.3 Role of mass movements in the evolution of the MSE*

279 The evolution of the MSE in the study area appears to have been determined by
 280 the interaction of: (i) fault activity associated with the tectonic regime of the cen-
 281 tral Mediterranean, (ii) sedimentary activity, driven by hemipelagic, pelagic and
 282 contouritic sedimentation, (iii) seafloor incision, related to bottom current activity
 283 and, possibly, to oceanographic and terrestrial processes that could have been ac-
 284 tive during sea level lowstands (e.g. Messinian Salinity Crisis). In this framework,
 285 the role of mass movements across the MSE and outer Malta Plateau was to erode
 286 the seafloor and transfer material to the lower MSE. What is interesting about our
 287 study area is that it presents a very good example of how mass movements and
 288 canyon processes are interrelated. Submarine mass movements control the extent

289 of lateral and headward extension of the canyons across the continental slope and
 290 shelf, as well as facilitate tributary development. They also remove material from
 291 the continental shelf and slope, feeding sediment and driving its transport down-
 292 canyon. Because of their size and position in the stratigraphic record, we believe
 293 that the mapped submarine mass movements do not constitute a significant geo-
 294 hazard to the central Mediterranean region.

295 5. References

- 296 Adam J, Reuther CD, Grasso M et al. (2000) Active fault kinematics and crustal stresses along the
 297 Ionian margin of southeastern Sicily. *Tectonophysics* 326: 217-239.
- 298 Argnani A, Bonazzi C (2005) Malta Escarpment fault zone offshore eastern Sicily: Pliocene-
 299 Quaternary tectonic evolution based on new multichannel seismic data. *Tectonics* 24: TC4009.
- 300 Casero P, Cita MB, Croce M et al. (1984) Tentative di interpretazione evolutiva della scarpata di Malta
 301 basata su dati geologici e geofisici. *Mem Soc Geol Ital* 27: 233-253.
- 302 Gardiner W, Grasso M, Sedgeley D (1995) Plio-Pleistocene fault movement as evidence for mega-
 303 block kinematics within the Hyblean-Malta Plateau, Central Mediterranean. *J Geodyn* 19: 35-51.
- 304 Grasso M (1993) Pleistocene structures along the Ionian side of the Hyblean Plateau (SE Sicily):
 305 Implications for the tectonic evolution of the Malta Escarpment, in: Max, M.D., Colantoni, P. (Eds.),
 306 UNESCO Technical Reports in Marine Science, Urbino, pp. 49-54.
- 307 Imbrie J, McIntyre A, Mix AC (1989) Oceanic response to orbital forcing in the Late Quaternary:
 308 Observational and experimental strategies, in: Berger, A. et al. (Eds.), *Climate and Geosciences: A*
 309 *Challenge for Science and Society in the 21st Century*. Reidel Publishing Company.
- 310 IOC, IHO, BODC (2003) Centenary Edition of the GEBCO Digital Atlas, in: Organisation, I.H. (Ed.),
 311 *General Bathymetric Chart of the Oceans*. British Oceanographic Data Centre, Liverpool.
- 312 Jongasma D, Van Hinte JE, Woodside JM (1985) Geologic structure and neotectonics of the north
 313 African continental margin south of Sicily. *Mar Petrol Geol* 2: 156-177.
- 314 Marani M, Argnani A, Roveri M et al. (1993) Sediment drifts and erosional surface in the central
 315 Mediterranean: Seismic evidence of bottom-current activity. *Sediment Geol* 82: 207-220.
- 316 Max MD, Kristensen A, Michelozzi E (1993) Small scale Plio-Quaternary sequence stratigraphy and
 317 shallow geology of the west-central Malta Plateau, in: Max, M.D., Colantoni, P. (Eds.), UNESCO
 318 Technical Reports in Marine Science, Urbino, pp. 117-122.
- 319 Micallef A, Masson DG, Berndt C et al. (2007) Morphology and mechanics of submarine spreading: A
 320 case study from the Storegga Slide. *J Geophys Res* 112: F03023.
- 321 Micallef A, Berndt C, Debono G (2011) Fluid flow systems of the Malta Plateau, Central
 322 Mediterranean Sea. *Mar Geol* 284: 74-85.
- 323 Micallef A, Mountjoy JJ, Canals M et al. (2012) Deep-seated bedrock landslides and submarine
 324 canyon evolution in an active tectonic margin: Cook Strait, New Zealand., in: Yamada, Y. et al.
 325 (Eds.), *Submarine Mass Movements and Their Consequences*. Springer, London, pp. 201-212.
- 326 Mulder T, Ducassou E, Gillet E et al. (2012) Canyon morphology on a modern carbonate slope of the
 327 Bahamas: Evidence of regional tectonic tilting. *Geology* 40: 771-774.

- 328 Osler J, Algan O (1999) A high resolution seismic sequence analysis of the Malta Plateau, Saclantcen
329 Report.
- 330 Rebesco M, Stow DAV (2001) Seismic expression of contourites and related deposits: A preface. *Mar*
331 *Geophys Res* 22: 303-308.
- 332 Scandone P, Patacca E, Radoicic R et al. (1981) Mesozoic and Cenozoic rocks from Malta Escarpment
333 (Central Mediterranean). *Am Assoc Petr Geol B* 65: 1299-1319.
- 334 Stow DAV, Faugetes JC, Howe JA et al. (2002) Bottom currents, contourites and deep-sea sediment
335 drifts: Current state-of-the-art, in: Stow, D.A.V. et al. (Eds.), *Deep-water contourite systems: Modern*
336 *drifts and ancient series, seismic and sedimentary characteristics*. Geological Society, London, pp. 7-
337 20.
- 338 ten Brink US, Geist EL, Lynett P et al. (2006) Submarine slides north of Puerto Rico and their tsunami
339 potential, in: Mercado, A., Liu, P.L.F. (Eds.), *Caribbean Tsunami Hazard*.
- 340 Tonarelli B, Turgutcan F, Max MD et al. (1993) Shallow sediments at four localities on the Sicilian-
341 Tunisian Platform, in: Max, M.D., Colantoni, P. (Eds.), *UNESCO Technical Reports in Marine*
342 *Science, Urbino*, pp. 123-128.
- 343
344 **Acknowledgments.** This research was supported by funding from the European Union 7th
345 Framework Programme (FP7/2007-2013) under grant agreements n° 228344 (EUROFLEETS),
346 n° 252702 (CAGE), n° 29874 (Geo-Habit) and ERC Starting Grant n° 258482 (CODEMAP).
347 Additional funding was provided by the Crown Research Institute Core funding to NIWA and
348 from the Griffith Geoscience Awards of the Department of Communications, Energy and Natu-
349 ral Resources under the National Geoscience Programme 2007–2013 of Ireland. We are
350 indebted to the CUMECS shipboard party, the captain, crew and technicians of *RV Urania*, and
351 to Suzanne Maclachlan and Jeremy Sothcott for their assistance with core analyses. Federica
352 Foglini, Jan Sverre Laberg and Sebastian Krastel are thanked for their insightful reviews.